Finite-size scaling analysis of the $S=1$ Ising model on the triangular lattice

Joseph B. Collins*
Department of Physics and Center for Advanced Computational Science, Temple University, Philadelphia, Pennsylvania 19122

Per Arne Rikvold
ChemLink Industrial/Petroleum Chemicals Division, Malvern, Pennsylvania 19355
and Department of Physics, Supercomputer Computations Research Institute, and Center for Materials Research and Technology, Florida State University, Tallahassee, Florida 32306

E. T. Gawlinski
Department of Physics and Center for Advanced Computational Science, Temple University, Philadelphia, Pennsylvania 19122
(Received 25 November 1987)

We study the $S=1$ Ising model, equivalent to the three-state lattice-gas model, with nearest-neighbor, pairwise interactions on a two-dimensional, triangular lattice. We pay particular attention to the antiferromagnetic phase diagrams. We show its relation to other well-studied models ($S=\frac{1}{2}$ Ising, Blume-Capel, Blume-Emery-Griffiths), classify the ground states, and calculate finite-temperature phase diagrams using transfer matrices and finite-size scaling for infinite strips of three and six sites width. The phase diagrams are quite complicated, with surfaces of first- and second-order transitions that intersect along lines of multicritical points of various kinds, providing a rich laboratory for studying a number of first-order phase transitions, critical and multicritical phenomena within the framework of one single model.

I. INTRODUCTION

Transfer-matrix methods applied to finite systems and finite-size scaling theory have been used with great success to study the critical properties of Ising and lattice-gas models.[1-4] Experience has shown that transfer-matrix models give numerical data for simple spin systems that rapidly converge, as a function of increasing system size, to the infinite system values. These data, e.g., the free energy, converge so rapidly, especially away from critical regions, that we may often assume that the results for small systems give reasonably accurate approximations to corresponding data for infinite systems. The use of finite-size scaling to determine the position of critical surfaces rounds out the calculational repertoire available for practical modeling and understanding of adsorption systems. The practical limitations of using these techniques are generally determined by the size of the transfer matrix, which must be diagonalized. The size of the transfer-matrix depends on the multiplicity of spin states, number of interactions, and symmetries of the Hamiltonian. For these reasons most of the applications of these methods have been confined to two-state models. One should note, however, that the physical information, i.e., coverage, free energy, correlation lengths, etc., for values of the parameters in noncritical regions is well approximated by even the smallest of strip widths for systems with infinite-length strips. In this way good results may be obtained for the phase diagrams for more complicated and physically interesting systems.

The model we analyze here has itself a multitude of possible phase diagrams with topologies dependent on the values of the parameters in the model Hamiltonian. In particular, we consider the $S=1$ Ising model (three-state lattice-gas) that we have used elsewhere as a model (Rikvold *et al.*[5]) for multicomponent adsorption problems and for which we have obtained adsorption isotherm data having a good correlation with an experimental system. The resulting phase diagrams are quite complicated and, in general, consist of surfaces of first- and second-order phase transitions that intersect along lines of multicritical points. We find that this most general nearest-neighbor $S=1$ Ising model provides an unusually rich laboratory for studying a number of phase transitions, critical, and multicritical phenomena within the framework of one single model.

In addition to the intrinsic interest due to its statistical-mechanical and thermodynamic richness, the $S=1$ Ising model is useful as a representation of a variety of physical and chemical systems. Some of these applications that have been suggested in the past include the classical papers by Blume and Capel on magnetic and electric phase transitions in crystals with local triplet states,[6] the λ transition, and phase separation in ^{3}He-^{4}He mixtures,[7] interfacial wetting in three-phase systems,[8] conformational phase transitions in amphiphilic monolayers at liquid-gas interfaces,[9,10] binary alloys in equilibrium with a gas,[11] microemulsions,[12] and multicomponent adsorption.[5,13,14] We do not intend this list of applications to be exhaustive, but merely to indicate the model's wide applicability, and possibly to act as an inspiration for its application to new problems.

II. THE $S=1$ ISING MODEL

We start with a Hamiltonian, Eq. (2.1), which, with five interaction constants, is the most general form of the Hamiltonian for an $S=1$ Ising model with nearest-neighbor, pairwise interactions.

 ©1988 The American Physical Society

$$\mathcal{H}=-J\sum_{\langle i,j\rangle}p_ip_j-K\sum_{\langle i,j\rangle}q_iq_j$$
$$-L\sum_{\langle i,j\rangle}(q_ip_j+p_iq_j)+D\sum_i q_i-H\sum_i p_i\ , \qquad (2.1)$$

where the Ising spins are $p_i\in\{-1,0,+1\}$ and $q_i=p_i^2$. The sums are $\sum_{\langle i,j\rangle}$ over nearest neighbors and $\sum_i$ over all lattice sites. The macroscopic densities conjugate to H and $-D$ will be denoted respectively by $P=N^{-1}\sum_i p_i$ and $Q=N^{-1}\sum_i q_i$. The parameters J and H are analogous to the usual interaction constant and field for the $S=\frac{1}{2}$ Ising model with $J>0$ corresponding to the ferromagnetic case. The field D distinguishes between zero and nonzero p_i with $D<0$ denoting a preference for $q_i=1$. Positive values of K correspond to a preference for nearest-neighbor spins being either $+1$ or -1, irrespective of sign, whereas $K<0$ indicates a preference for bonds involving at least one zero spin. Positive values of the coupling term L correspond to a preference for ferromagnetic ordering with all $p_i=+1$. The Hamiltonian is invariant under the transformation ($L\rightarrow -L$, $H\rightarrow -H, p_i\rightarrow -p_i$). The actual structures of the ordered phases and the nature of the phase transitions that separate them depend on the interplay between these five parameters, the symmetry of the underlying lattice, and the temperature, as discussed in detail in Secs. IV–VI. We have chosen for our model the triangular lattice, corresponding to (a) various sets of adsorption sites on the $\{111\}$ planes of a three-dimension face-centered-cubic lattice, (b) close packing of equal-sized spheres on a plane surface, or (c) adsorption sites on the basal plane of graphite.

This model is related to previously studied models of a simpler nature. For $K=L=0$ it reduces to the Blume-Capel model,[6] and for $L=0$ to the Blume-Emery-Griffiths (BEG) model.[7] These special cases have been studied previously by renormalization-group techniques,[15–17] domain-wall calculations and Monte Carlo simulations,[8] mean-field approximations,[6,7,9–12] and transfer-matrix finite-size scaling techniques.[2,18] The majority of these studies are concerned with the ferromagnetic model on a square of simple-cubic lattice. The most comprehensive study of phase diagrams for the antiferromagnetic case seems to be Saito's mean-field calculation on a simple-cubic lattice.[11] Two-component adsorption on the square lattice has been studied by Huckaby and Kowalski,[13] who performed a full ground-state calculation, and by Lee and Landau, who performed a Monte Carlo simulation.[14] Recently Lee *et al.*, have studied the effects of domain-wall excitations in the antiferromagnetic XY model on a triangular lattice.[14]

III. THREE-STATE LATTICE-GAS MODEL

The $S=1$ Ising model (in the canonical ensemble) described above is related to the three-state (A, B, and a vacancy or solvent particle) lattice-gas model in a manner analogous to the relation between and the $S=\frac{1}{2}$ Ising model and a two-state lattice-gas model.[1,14] In this more complex model, a three-state, nearest-neighbor lattice gas, adsorbate particles of two species, A and B, may occupy the sites of a two-dimensional lattice representing the absorbent surface. If the model is interpreted to represent adsorption from a binary gas, a site that is occupied by neither A nor B is considered vacant. It it is alternatively interpreted to represent adsorption from a solution of A and B in a solvent, then the third state represents a site occupied by a solvent particle. The latter physical situation is considerably more complicated than the former and, although encouraging experimental results have recently been reported,[19,20] we do not expect it to be more than qualitatively described by this simplest and most general three-state model. The lattice-gas Hamiltonian for this model (in the grand-canonical ensemble) is

$$\mathcal{H}_{\rm LG}-\mu_A\theta_A N-\mu_B\theta_B N=-\phi_{AA}\sum_{\langle i,j\rangle}c_i^Ac_j^A$$
$$-\phi_{AB}\sum_{\langle i,j\rangle}(c_i^Ac_j^B+c_i^Bc_j^A)$$
$$-\phi_{BB}\sum_{\langle i,j\rangle}c_i^Bc_j^B$$
$$-\mu_A\sum_i c_i^A-\mu_B\sum_i c_i^B\ , \qquad (3.1)$$

where the adsorption state of the ith lattice site is given by the local concentration variables c_i^A and c_i^B. The local concentration of A, c_i^A, equals unity if the site is occupied by an A particle and vanishes otherwise. The local concentration of B, c_i^B, behaves analogously. Any site can be occupied by at most one particle, so that $c_i^Ac_i^B=0$. The change in chemical potential when one X particle is removed from the bulk phase and adsorbed on the surface is $-\mu_X$ (defined to include the binding energy relative to the bulk phase). The total number of lattice sites is N, and the density conjugate to μ_X is $\theta_X=N^{-1}\sum_i c_i^X$, the surface coverage by species X. The interaction energies ϕ_{AA}, ϕ_{BB}, and ϕ_{AB} describe effective interactions between particles adsorbed on the surface. In general they depend on the substrate, and their determination from first principles would demand quantum-mechanical calculations beyond the scope of the present work.[21] These interaction energies, in general, may bear little or no relation to the interaction energies between the same particles in the bulk phase. The sign convention is such that $\phi_{XY}>0$ denotes an effective attraction and $\mu_X>0$ denotes a tendency for adsorption in the absence of adsorbate-adsorbate interactions. In terms of a liquid solution interpretation, all the interaction strengths and chemical potentials are considered relative to the state in which both the adsorbent surface and the adsorbate particles are completely solvated.

The local concentration variables c_i^A and c_i^B are related to the Ising variables by a linear combination

$$c_i^A=\tfrac{1}{2}(q_i+p_i)\ , \qquad (3.1a)$$

$$c_i^B=\tfrac{1}{2}(q_i-p_i)\ . \qquad (3.1b)$$

The interaction constants are related to those of the Ising model by

$$\phi_{AA}=J+K+2L\ ,$$
$$\phi_{BB}=J+K-2L\ ,$$
$$\phi_{AB}=K-J\ ,$$
$$\mu_A=H-D\ , \tag{3.2a}$$
$$\mu_B=-H-D\ ,$$

or, equivalently,

$$J=\tfrac{1}{4}(\phi_{AA}-2\phi_{AB}+\phi_{BB})\ ,$$
$$K=\tfrac{1}{4}(\phi_{AA}+2\phi_{AB}+\phi_{BB})\ ,$$
$$L=\tfrac{1}{4}(\phi_{AA}-\phi_{BB})\ , \tag{3.2b}$$
$$D=-\tfrac{1}{2}(\mu_A+\mu_B)\ ,$$
$$H=\tfrac{1}{2}(\mu_A-\mu_B)\ .$$

Thus $p_i=1$ means $c_i^A=1$, $p_i=-1$ means $c_i^B=1$, and $p_i=0$ means $c_i^A=c_i^B=0$. Note that $q_i=c_i^A+c_i^B$ is the total local concentration variable. A preference for AA bonds over BB bonds is indicated by $L>0$. Positive H denotes a preference for single-particle adsorption of A over B, and negative D corresponds to a preference for high total coverage. As we further discuss the model we shall refer alternatively to either lattice-gas or Ising notation.

IV. ORDERED STATES AND GROUND-STATE CALCULATIONS

Those ordered states on the triangular lattice that can be reached by second-order phase transitions are determined by Landau-Lifshitz group-theoretical arguments. The method is described in detail in the standard Ref. 22, and the results are as follows: The lattice symmetry group is p6mm, which, in addition to the identity representation, has one two-dimensional, and one three-dimensional representation. The ordered states generated by the two-dimensional representation are denoted $(\sqrt{3}\times\sqrt{3})$ and correspond to a separation of the lattice into three equivalent sublattices. The primitive unit cell contains three sites, one from each sublattice, as shown in Fig. 1. The ordered states generated by the three-dimensional representation are denoted (2×2), and correspond to a separation of the lattice into four equivalent sublattices. The primitive unit cell contains four sites, one from each sublattice. Disordered states, denoted (1×1), are generated by the identity representation. Specific states are identified by their corresponding values of P and Q as $(XxY)_P^Q$. The energy per lattice site of any specific state is obtained by evaluating the Hamiltonian for the corresponding configuration. Which one of these states is the actual ground state depends on the values of the five parameters, J, K, L, D, and H, in the Hamiltonian. The boundaries between the regions in this five-dimensional parameter space that correspond to a particular ground state are obtained by pairwise equating the ground-state energies. The ground states are uniform in the asymptotic strong-field limits. For large positive H the ground state is $(1\times1)_1^1$, for large negative H it is $(1\times1)_{-1}^1$, and for large positive D it is $(1\times1)_0^0$. Proceeding from each asymptotic strong-field region towards one of the other two, we determine which of the ordered states first becomes lower in energy than the uniform state. In case of degeneracies between several ordered states, we then determine which one of these has the lower energy as the fields are weakened further. The values of the fields H and D that mark the transition lines between different ground states depend on the coupling constants J, K, and L. Different values of the coupling constants therefore lead to different ground-state diagrams in the H,D plane, as discussed in detail below. The ground-state calculation described above is straightforward, but rather tedious. The result is that for the general $S=1$ Ising model represented by the nearest-neighbor Hamiltonian, Eq. (2.1), on a triangular lattice only (1×1) and $(\sqrt{3}\times\sqrt{3})$ states are realized as ground states. These ground states together with their corresponding values of Q, P, θ_A, θ_B, and energy per lattice site are listed in Table I. The (2×2) states do not result in ground states except for being degenerate with (1×1) or $(\sqrt{3}\times\sqrt{3})$ states along certain phase-boundary lines at zero temperature. We choose the notation for identifying ground states as $(1\times1)_P^Q$ for disordered phases and $(\sqrt{3}\times\sqrt{3})_P^Q$ for the ordered phases.

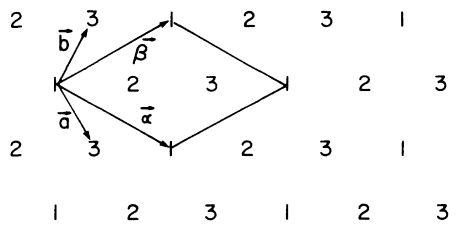

FIG. 1. Triangular lattice with primitive lattice vectors **a** and **b**. The three sublattices corresponding to the $(\sqrt{3}\times\sqrt{3})$ ordered states are marked 1, 2, and 3, respectively, and the $(\sqrt{3}\times\sqrt{3})$ unit vectors are $\boldsymbol{\alpha}$ and $\boldsymbol{\beta}$.

We redefine the temperature in units of $k_BT/|J|$ and introduce the reduced coupling constants $j=J/|J|$, $k=K/|J|$, $l=L/|J|$, $d=D/|J|$, and $h=H/|J|$. Examination of the ground states for various values of j, k, and l show that transitions between certain phases may or may not exist, depending on the topology of the ground-state diagram. Our calculation shows that in terms of the fields d and h the model has 32 possible topologically different ground-state diagrams, the features of which depend on the values of the interaction constants j, k, and l.

The first level of classification distinguishes between the ferromagnetic $(j=+1)$ and the antiferromagnetic $(j=-1)$ cases. For both ferromagnetic and antiferromagnetic systems the k,l plane is divided into four main regions, I–IV. The defining inequalities of these four regions are given in Table II, both in Ising and lattice-gas terms. As noted by Saito,[11] the defining relations are particularly simple in lattice-gas language, depending only on the homonuclear interactions ϕ_{AA} and ϕ_{BB}: region I corresponds to both ϕ_{AA} and ϕ_{BB} attractive, II corre-

TABLE I. Ground states of nearest-neighbor $S=1$ Ising model on triangular lattice. An * denotes states that may only be realized as ground states in the antiferromagnetic case, $J<0$.

State	Config.	Q	P	θ_A	θ_B	Degeneracy	Energy per lattice site
$(1\times1)^1_1$	$\begin{matrix}A\\AA\end{matrix}$	1	1	1	0	1	$-3J-3K-6L+D-H$
$(1\times1)^1_{-1}$	$\begin{matrix}B\\BB\end{matrix}$	1	−1	0	1	1	$-3J-3K+6L+D+H$
$(1\times1)^0_0$	$\begin{matrix}O\\OO\end{matrix}$	0	0	0	0	1	0
$*(\sqrt{3}\times\sqrt{3})^1_{1/3}$	$\begin{matrix}B\\AA\end{matrix}$	1	$\frac{1}{3}$	$\frac{2}{3}$	$\frac{1}{3}$	3	$J-3K-2L+D-\frac{1}{3}H$
$*(\sqrt{3}\times\sqrt{3})^1_{-1/3}$	$\begin{matrix}A\\BB\end{matrix}$	1	$-\frac{1}{3}$	$\frac{1}{3}$	$\frac{2}{3}$	3	$J-3K+2L+D+\frac{1}{3}H$
$(\sqrt{3}\times\sqrt{3})^{2/3}_{2/3}$	$\begin{matrix}O\\AA\end{matrix}$	$\frac{2}{3}$	$\frac{2}{3}$	$\frac{2}{3}$	0	3	$-J-K-2L+\frac{2}{3}D-\frac{2}{3}H$
$(\sqrt{3}\times\sqrt{3})^{2/3}_{-2/3}$	$\begin{matrix}O\\BB\end{matrix}$	$\frac{2}{3}$	$-\frac{2}{3}$	O	$\frac{2}{3}$	3	$-J-K+2L+\frac{2}{3}D+\frac{2}{3}H$
$*(\sqrt{3}\times\sqrt{3})^{2/3}_0$	$\begin{matrix}O\\AB\end{matrix}$	$\frac{2}{3}$	0	$\frac{1}{3}$	$\frac{1}{3}$	6	$J-K+\frac{2}{3}D$
$(\sqrt{3}\times\sqrt{3})^{1/3}_{1/3}$	$\begin{matrix}O\\AO\end{matrix}$	$\frac{1}{3}$	$\frac{1}{3}$	$\frac{1}{3}$	0	3	$\frac{1}{3}D-\frac{1}{3}H$
$(\sqrt{3}\times\sqrt{3})^{1/3}_{-1/3}$	$\begin{matrix}O\\BO\end{matrix}$	$\frac{1}{3}$	$-\frac{1}{3}$	0	$\frac{1}{3}$	3	$\frac{1}{3}D+\frac{1}{3}H$

sponds to ϕ_{AA} attractive and ϕ_{BB} repulsive, III corresponds to ϕ_{AA} repulsive and ϕ_{BB} attractive, and IV corresponds to both ϕ_{AA} and ϕ_{BB} repulsive. The remaining subdivisions of the two k,l planes result from the toplogically distinct ways in which the ground states extending from the three asymptotic regions (described in Sec. V) in the h,d plane intersect. In Fig. 2(a) are shown the seven regions in the k,l plane that correspond to topologically distinct ground-state diagrams for the ferromagnetic case. The k,l plane with 25 regions corresponding to topologically distinct antiferromagnetic ground-state diagrams are shown in Fig. 2(b).

The general difference between the ferromagnetic and antiferromagnetic ground-state diagrams can easily be seen by considering the large, negative d behavior of the model. In this region the Hamiltonian reduces to a $S=\frac{1}{2}$ Ising model (see Sec. V). For $j=+1$ there is a ferromagnetic Ising transition from $(1\times1)^1_{-1}$ to $(1\times1)^1_1$ at $h=-6l$ in the h,d plane. On the other hand, for $j=-1$ there are two $(\sqrt{3}\times\sqrt{3})^1_{\pm1/3}$ ground states between the $(1\times1)^1_{-1}$ and $(1\times1)^1_1$ regions symmetric about the same line, $h=-6l$, in the h,d plane. These $(\sqrt{3}\times\sqrt{3})^1_{\pm1/3}$ states are just the usual states expected for a $S=\frac{1}{2}$ Ising antiferromagnet on a triangular lattice.

TABLE II. Main regions in the (k,l) plane.

Region	Ising condition	Lattice-gas condition
I	$-k-j<2l<k+j$	$\phi_{AA}>0$ and $\phi_{BB}>0$
II	$2l>-k-j$ and $2l>k+j$	$\phi_{AA}>0$ and $\phi_{BB}<0$
III	$2l<-k-j$ and $2l<k+j$	$\phi_{AA}<0$ and $\phi_{BB}>0$
IV	$k+j<2l<-k-j$	$\phi_{AA}<0$ and $\phi_{BB}<0$

The four major subregions of the k,l diagrams for either $j=\pm1$ correspond similarly to the asymptotic behavior for either large $-\mu_A$ or for large $-\mu_B$. In either case the Hamiltonian, Eq. (3.2), again reduces to a $S=\frac{1}{2}$ Ising model. For large $-\mu_A$ this results in a phase diagram that is symmetric about the line $\mu_B=-3J-3K+6L=-3\phi_{BB}$. For large $-\mu_B$ this results in a phase diagram symmetric about the line $\mu_A=-3J-3K-6L=-3\phi_{AA}$. Each of these two asymptotic regions may independently be ferromagnetic or antiferromagnetic, depending on k and l, leading to four possible combinations of asymptotic behavior in the $-\mu_A,-\mu_B$ directions considered together.

V. ASYMPTOTIC RESULTS

In the asymptotic, strong-field limits the Hamiltonian, Eq. (3.2), reduces to that of the well-studied $S=\frac{1}{2}$ Ising model with nearest-neighbor, pairwise interactions on a triangular lattice,

$$\hat{\mathcal{H}}=-\hat{J}\sum_{\langle i,j\rangle}\sigma_i\sigma_j-\hat{H}\sum_i\sigma_i\ . \tag{5.1}$$

The well-studied characteristics of the phase surfaces in these regions are noted below, and are important to consider since we expect the phase diagrams for the intermediate field strengths to smoothly approach the asymptotic configurations. As $D\to-\infty$ the state $p_i=0$ becomes energetically unfavorable, and the effective $S=\frac{1}{2}$ Ising model is defined by

$$\sigma_i = p_i = \pm 1 \ ,$$
$$\hat{J} = J \ , \qquad (5.2a)$$
$$\hat{H} = H + 6L \ .$$

As $H \to +\infty$, and $D \to +\infty$ ($\mu_B \to -\infty$), then $p_i = -1$ (corresponding to adsorbed B atoms) becomes unfavorable. Thus $p_i \to q_i$, and the model reduces to the two-state lattice-gas model for single-component adsorption of A. The corresponding effective $S = \frac{1}{2}$ Ising model is defined by

$$\sigma_i = 2q_i - 1 \ ,$$
$$\hat{J} = \tfrac{1}{4}(J + K + 2L) = \tfrac{1}{4}\phi_{AA} \ , \qquad (5.2b)$$
$$\hat{H} = \tfrac{1}{2}[(H - D) + 3(J + K + 2L)] = \tfrac{1}{2}(\mu_A + 3\phi_{AA}) \ .$$

Analogously, as $H \to -\infty$ and $D \to +\infty$ ($\mu_A \to -\infty$), then $p_i \to -q_i$, i.e., adsorbed A becomes unfavorable and the model reduces to the two-state lattice-gas model for adsorption of B. The corresponding effective $S = \frac{1}{2}$ Ising parameters for this asymptotic limit are

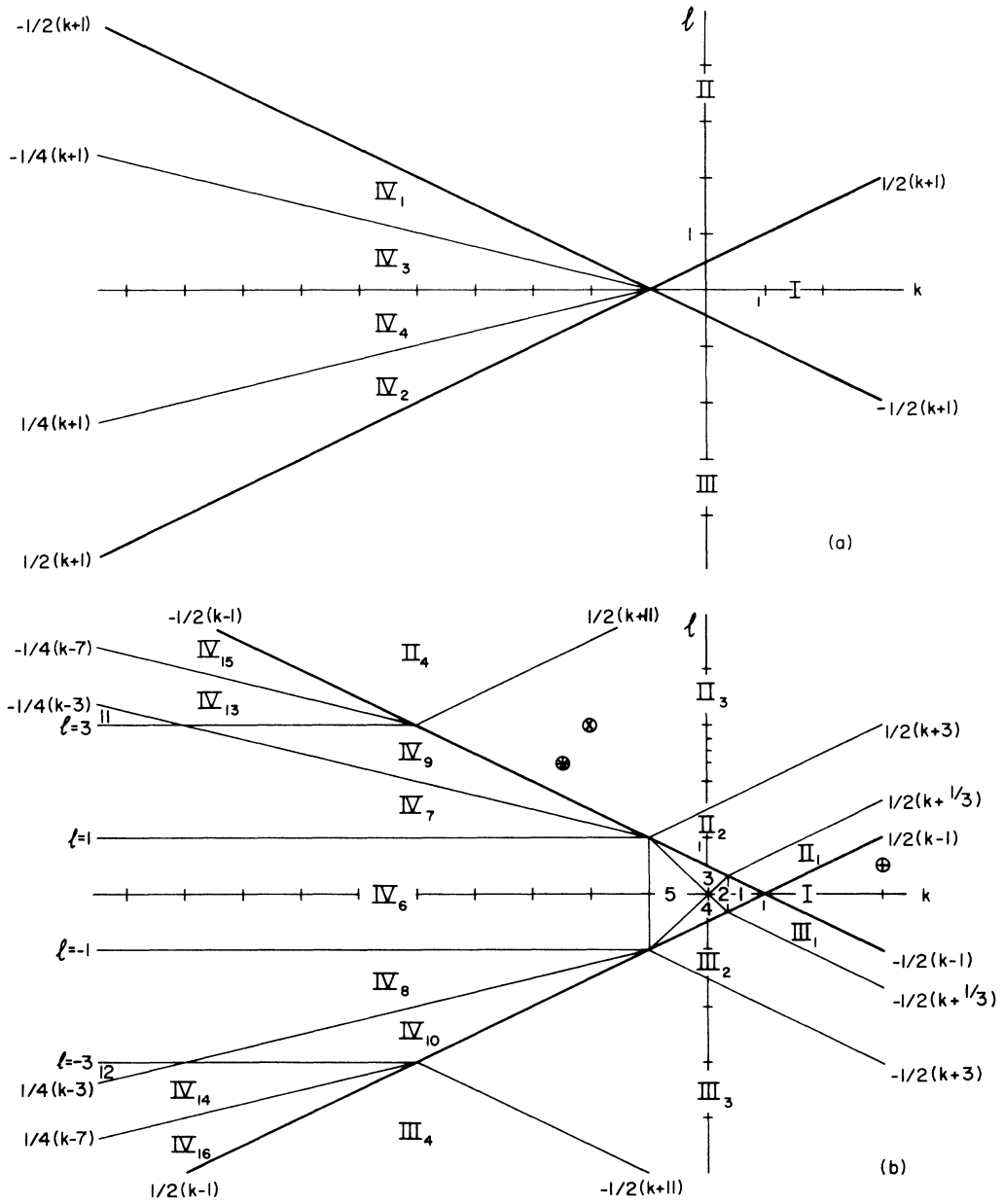

FIG. 2. (a) The seven regions in the k,l plane that correspond to topologically distinct ground-state diagrams for the ferromagnetic case, $j = +1$. (b) The 25 regions in the k,l plane that correspond to topologically distinct ground-state diagrams for the antiferromagnetic case, $j = -1$.

$$\sigma_i = 2q_i - 1 ,$$
$$\hat{J} = \tfrac{1}{4}(J + K - 2L) = \tfrac{1}{4}\phi_{BB} , \tag{5.2c}$$
$$\hat{H} = \tfrac{1}{2}[-(H + D) + 3(J + K - 2L)] = \tfrac{1}{2}(\mu_B + 3\phi_{BB}) .$$

Previous studies of the $S = \frac{1}{2}$ Ising model on the triangular lattice thus give us points of comparison in these asymptotic limits, namely the positions and characteristics of the phase-transition surfaces.

In the ferromagnetic (FM) case, $\hat{J} > 0$, the $S = \frac{1}{2}$ Ising model on a triangular lattice has a first-order phase transition at $\hat{H} = 0$. The line of the first-order transitions terminates at the exactly known[23] critical temperature for the triangular lattice, $k_B \hat{T}_c^{\mathrm{FM}}/\hat{J} = 4/(\ln 3) = 3.640\ldots$, which point has, of course, the usual Ising critical properties.

In the antiferromagnetic case, $\hat{J} < 0$, the ground state of the $S = \frac{1}{2}$ Ising model at $\hat{H} = 0$ is infinitely degenerate with a finite entropy at zero temperature.[24] There is therefore no phase transition at zero field and finite temperature. The general shape of the $\hat{H}, T$ phase diagram was first conjectured by Domb.[25] The critical surface takes the shape of two humps that come to zero at $\hat{H} = 0, \pm 6|\hat{J}|$, and which are symmetric about $\hat{H} = 0$, since this Hamiltonian, Eq. (5.1), is invariant under the transformation $\hat{H} \to -\hat{H}$, $\sigma_i \to -\sigma_i$. For $\hat{H} = 0$ the antiferromagnetic $S = \frac{1}{2}$ model is expected to belong to the universality class of the XY model with a phase transition at $T = 0$ and a thermal exponent $y_T = 0$.[23] At the same point the slope of the line of critical points versus $\hat{H}$ is expected to be infinite, based on scaling arguments.[3] For $0 < \hat{H} < 6|\hat{J}|$ the ground state is $(\sqrt{3}\times\sqrt{3})^{\frac{1}{3}}_{\frac{1}{3}}$, and for $\hat{H} > 6|\hat{J}|$ it is $(1\times 1)^{\frac{1}{1}}_{1}$. For all nonzero fields the antiferromagnetic $S = \frac{1}{2}$ Ising model belongs to the universality class of the three-state Potts model,[26] with thermal exponent $y_T = \frac{6}{5}$. At $\hat{H} = \pm 6|\hat{J}|$ and $T = 0$ is identical to the exactly solved hard-hexagon model.[27] The slope versus field of the line of the critical points is related to the critical fugacity of the latter,[28] and given by $-2/ln[\frac{1}{2}(11 + 5\sqrt{5})] = -0.8312\ldots$. The behavior of the line of critical points for fields in the range $0 < \hat{H} < 6|\hat{J}|$ has been well studied by a variety of methods, including Monte Carlo simulation,[29] the finite-size scaling transfer matrix method,[3] and variational approximations.[30] These methods all give a maximum value of the antiferromagnetic critical temperature in the range $1.33|\hat{J}|$ to $1.40|\hat{J}|$, occurring at $\hat{H} = \pm 3|\hat{J}|$. Our numerical results give, for the relevant asymptotic regions, a maximum antiferromagnetic critical temperature of $1.33|\hat{J}|$ and values for the whole critical surface which are in good agreement with previous finite-size scaling results for the $S = \frac{1}{2}$ Ising model.[3]

VI. TRANSFER MATRIX RESULTS AT FINITE TEMPERATURES—PHASE DIAGRAMS

We have obtained thermodynamic data for the $S = 1$ model at finite temperatures and finite fields using the transfer matrix method[31] and finite-size scaling.[32] In the usual fashion a system in the shape of an infinitely long strip was partitioned into layers of width N, parallel to one of the primitive vectors of the triangular lattice. The transfer matrix was block-diagonalized utilizing the invariance of the Hamiltonian under one-step translations in the direction parallel to the layers, represented by the unitary operator $\underline{U}_N$, which is cyclic with period N. It can be shown that, for this particular model, the block $\underline{T}^S$, corresponding to states invariant under $\underline{U}_N$, is a real, symmetric matrix. Operators corresponding to the single-layer $(\sqrt{3}\times\sqrt{3})$ order parameter transform under $\underline{U}_N$ with a phase factor $e^{i2\pi/3}$. The $(\sqrt{3}\times\sqrt{3})$ order parameter correlation lengths are therefore given by the eigenvalues of the block $\underline{T}^3$, corresponding to eigenvectors of $\underline{U}_N$ with eigenvalue $e^{i2\pi/3}$. For this particular model $\underline{T}^3$ is proportional to a complex Hermitian matrix. The proportionality constant is a complex phase factor indicating threefold symmetry under translations in the direction parallel to the infinite strip. We have constructed the matrices $\underline{T}^S$ and $\underline{T}^3$ for strip widths $N = 3$ and $N = 6$ and diagonalized them using a Floating Point Systems Model 264 array processor with APMATH64 library routines RS and CH (based on EISPACK routines of the same name). The diagonalization results in three eigenvalues of interest. The largest eigenvalue of both $\underline{T}^S$ and the total transfer matrix $\underline{T}$ is λ_1^S. By virtue of the Perron-Frobenius theorem, it is positive and nondegenerate. The other two eigenvalues of interest are λ_2^S, second largest of $\underline{T}^S$, and λ_1^3, the eigenvalue of $\underline{T}^3$ with the greatest modulus. These two eigenvalues alternate as the second largest eigenvalues of the total transfer matrix.

These three eigenvalues give rise to two important lengths. The order-parameter correlation length for the $(\sqrt{3}\times\sqrt{3})$-ordered phase is identified as

$$\xi_N^3 \equiv (\ln|\lambda_1^S/\lambda_1^3|)^{-1} . \tag{6.1a}$$

A second length, the persistence length, is similarly defined

$$\xi_N^S \equiv (\ln|\lambda_1^S/\lambda_2^S|)^{-1} . \tag{6.1b}$$

Second-order phase transitions from the ordered phases to the disordered phases have been located by the Nightingale criterion[32]

$$\xi_N^3/N = \xi_{N'}^3/N' . \tag{6.2}$$

No second-order transitions exist between any two ordered phases since they are all of the same symmetry.

First-order transitions in this model involve discontinuities in P and Q when $N = \infty$. For a finite-size system this corresponds to a rapid variation in the region of the first-order transition. The position of the first-order transition can also be determined by the requirement that

$$\langle \lambda_1^S | \hat{Q} | \lambda_1^S \rangle = \langle \lambda_2^S | \hat{Q} | \lambda_2^S \rangle \tag{6.3}$$

in this region of rapid variation, where $\langle \lambda_n^S|$ and $|\lambda_n^S\rangle$ are the left and right eigenvectors corresponding to the eigenvalue λ_n^S of $\underline{T}^S$.[4]

This estimate converges exponentially with N to its infinite-system value, and the result for $N = 6$ is presum-

ably quite good. The single-layer operators $\hat{P}$ and $\hat{Q}$ that correspond to P and Q are invariant under $\underline{U}_N$. As pointed out by Bartelt *et al.*,[4] the size of the discontinuity in, e.g., Q can be estimated by fitting the eigenvalues $Q_N^{\pm}$ of the matrix

$$\begin{bmatrix} \langle \lambda_1^S | \hat{Q} | \lambda_1^S \rangle & \langle \lambda_1^S | \hat{Q} | \lambda_2^S \rangle \\ \langle \lambda_2^S | \hat{Q} | \lambda_1^S \rangle & \langle \lambda_2^S | \hat{Q} | \lambda_2^S \rangle \end{bmatrix} \tag{6.4}$$

to the form

$$Q_N^{\pm} = Q_{\infty}^{\pm} + aN^{-\beta/\nu} . \tag{6.5}$$

The width of the region of finite-size rounding where the off-diagonal elements in (6.4) are appreciably different from zero vanishes exponentially with N. It therefore introduces very little error to diagonalize (6.4) for both $N=6$ and $N=3$ at the value of the transition field determined from (6.3) with $N=6$. Since only two stripwidths are used, the ratio of critical indices β/ν must be determined from a knowledge of the universality class of the particular transition. As explained in Sec. V, the order-disorder first-order transitions in the present model have critical points in the universality class of the two-dimensional $S=\frac{1}{2}$ Ising model, which has $\beta=\frac{1}{8}$ and $\nu=1$. The temperature at which the discontinuity $Q_{\infty}^{+}-Q_{\infty}^{-}$ vanishes provides one estimate of the critical temperature for the first-order transition.

The persistence lengths for $N=3$ and $N=6$ give a second, consistent determination of both the first-order surface and its critical edge. The persistence length has a sharp peak, increasing as e^N, at the first-order transition. This peak readily determines the location of the transition. As one crosses the first-order transition close to the critical point ξ_6^S peaks much less sharply than at lower temperatures. At the point where $\xi_6^S/6=\xi_3^S/3$ become tangent at their peaks rather tan $\xi_6^S/6 \gg \xi_3^S/3$ below T_c, we interpret that the Nightingale criterion is being satisfied at the critical edge of the first-order surface. We find that our two determinations of critical temperatures at the edges of the first-order surfaces agree to within about 0.5%. Since the critical indices for the order-disorder and order-order first-order transitions are different universality classes the positions of the multicritical points have been determined solely by the persistence-length scaling method.

We provide our numerical data for phase-transition surfaces in graphical form with accompanying descriptions for two sample systems whose parameters allow for modeling enhanced (model E) and inhibited (model P, for poisoning) adsorption, as discussed in detail in Ref. 5. Their ground-state diagrams are shown in Fig. 3.

The first system, model E ($j=-1$, $k=3.0$, $l=0.5$), whose ground-state diagram is shown in Fig. 3(a), is particularly simple. We show a three-dimensional view of the shape of the field-temperature space phase diagram in Fig. 4(a) where the X, Y, and Z axes are h, d, and T, respectively. A double-humped surface of second-order transitions is illustrated with contours at constant d, and a "wall" of first-order transitions is represented by contours at constant h. In this system the second-order double hump of the effective two-state antiferromagnetic model for the asymptotic (large $-d$) region comes from large negative d into the intermediate region with little (a few percent) variation in magnitude and shape until it terminates in a line of critical endpoints at its intersection with the first-order "wall." This first-order surface separates the $(\sqrt{3}\times\sqrt{3})^{1}_{\pm 1/3}$ and $(1\times 1)^{1}_{\pm 1}$ phases from the $(1\times 1)^{0}_{0}$ phase. In the intermediate region this first-order surface rises vertically until it reaches its intersection with the second-order humps, whereupon it arches slightly towards positive d and terminates in a continuous

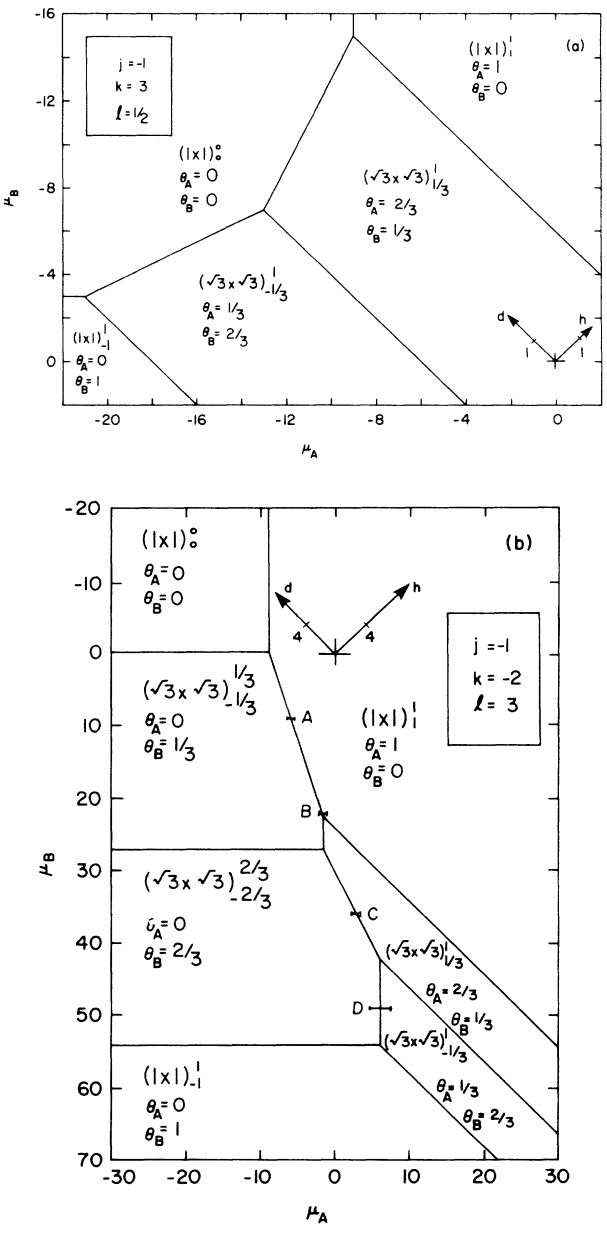

FIG. 3. (a) Ground-state diagram for model E ($j=-1$, $k=3.0$, $l=0.5$), which exhibits enhanced adsorption. (b) Ground-state diagram for model P ($j=-1$, $k=-2.0$, $l=3.0$), which exhibits inhibited adsorption (poisoning) of A by B. The horizontal bars labeled $A-D$ correspond to the cross sections shown in Fig. 5.

edge of critical points. As it extends towards either large $-\mu_B$ or *large* $-\mu_A$ this first-order surface stands vertically and its critical edge quickly approaches the asymptotic critical temperature for the equivalent, asymptotic, $S=\frac{1}{2}$ Ising model.

The second system, model P ($j=-1$, $k=-2.0$, $l=3.0$), whose ground state is shown in Fig. 3(b), is more complicated. We show a three-dimensional view of its shape in Fig. 4(b). Here there are two sets of double-humped, second-order surfaces; one extending from large negative d, since $j=-1.0$, and the other extending from large $-\mu_A$ corresponding to a negative ϕ_{BB}. Their cross sections quickly approach their asymptotic values. Extending from the large $-\mu_B$ region there is a first-order wall, corresponding to positive ϕ_{AA}, dividing the $(1\times1)^0_0$ phase from the $(1\times1)^1_1$ phase. We illustrate how this first-order wall progresses until it disappears at $d=-24.0$, $h=-18.0$ by taking cross sections of it, plotting it for μ_A versus T at selected values of μ_B, Fig. 5. The values of μ_B and ranges of μ_A for which these cross sections have been plotted are indicated by horizontal bars in Fig. 3(b). It is quite striking how small the region of the phase diagram is where the phase boundary surfaces deviate significantly from their asymptotic, limiting shapes. From between the $(1\times1)^0_0$ and $(1\times1)^1_1$ phases the first-order surface continues along to separate the $(\sqrt{3}\times\sqrt{3})^{1/3}_{-1/3}$ phase from the $(1\times1)^1_1$ phase, Figs. 5(a) and 5(b), and further still to separate the $(\sqrt{3}\times\sqrt{3})^1_{-1/3}$ and $(\sqrt{3}\times\sqrt{3})^{2/3}_{-2/3}$ phases from the $(\sqrt{3}\times\sqrt{3})^1_{1/3}$ phase, Fig. 5(c). It finally appears to vanish ($T_c\to0$) at the juncture of the $(\sqrt{3}\times\sqrt{3})^{2/3}_{-2/3}$, $(\sqrt{3}\times\sqrt{3})^1_{1/3}$, and $(\sqrt{3}\times\sqrt{3})^1_{-1/3}$ ground states. As μ_A is increased at constant μ_B at finite temperature, θ_A increases continuously giving no numerical evidence of a first or second-order transition between the $(\sqrt{3}\times\sqrt{3})^{2/3}_{-2/3}$ and $(\sqrt{3}\times\sqrt{3})^1_{-1/3}$ phases at finite temperature. We argue that the critical temperature for this transition is zero. For low temperatures this transition is effectively that of a noninteracting gas of A's, being isolated from each other by two sublattices full of B's. The critical temperature for such a transition is exactly zero. Since there is no symmetry change between these two ordered phases we also would not expect a second-order transition dividing the two phases at finite temperature. Consistent with this interpretation we find that the isotherms in this region agree exactly with the theoretical result for a noninteracting lattice-gas model for A with chemical potential (μ_A-6) (i.e., for noninteracting adsorption of A with reduced single-site binding energy due to the repulsive interaction with the B "cages"). Also consistent with this interpretation, the upper critical surfaces for these two phases are smoothly and continuously joined, as shown in Fig. 5(d).

In Fig. 5(a) the first-order line terminates at a critical point and meets the second-order line at a critical end point. In Fig. 5(b) the numerical accuracy is not sufficient to determine whether the first- and second-order lines join at a tricritical point or whether a critical point and a critical end point are located very close together. In Fig. 5(c) the first-order line seems to join one second-order line at a tricritical point and meets the other at a critical end point. Our present calculation does not afford sufficient numerical accuracy to determine the higher-order critical points that presumably exist where these clear-cut cases merge (at some value of μ_B between $\mu_B=9$ and $\mu_B=22$).

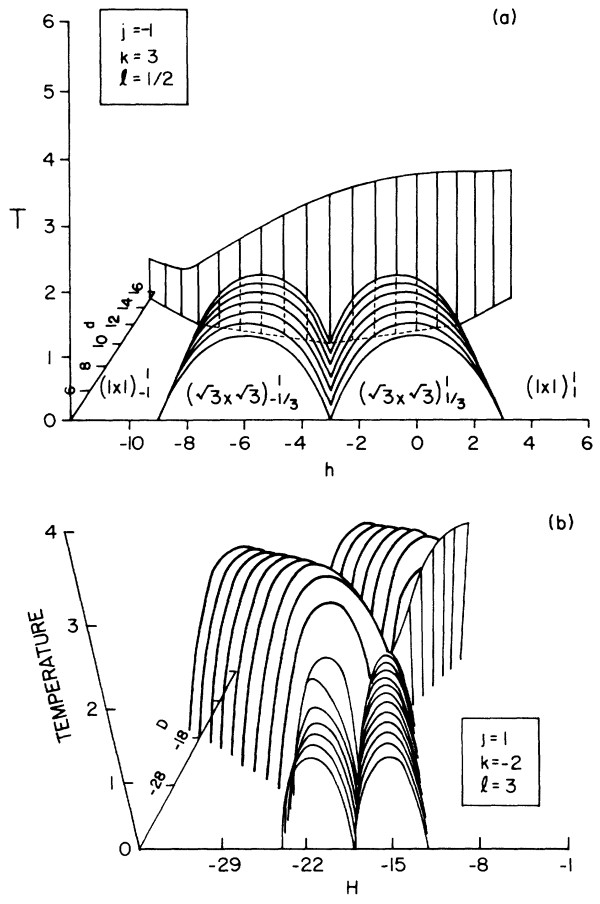

FIG. 4. (a) A three-dimensional view of the shape of the field-temperature space phase diagram for model E ($j=-1$, $k=3.0$, $l=0.5$), where the X, Y, and Z axes are h, d, and T, respectively. Two second-order humped surfaces are illustrated with contours at constant d, and a first-order "wall" is represented by contours at constant h. Further details are discussed in the text. (b) A three-dimensional view of the shape of the field-temperature phase diagram for model P ($j=-1$, $k=-2.0$, $l=3.0$), where the axes are the same as in a. There are two sets of second-order double-humped surfaces; one extending from large negative d, and the other extending from large $-\mu_A$. Extending from the large $-\mu_B$ region there is a first-order wall dividing the $(1\times1)^0_0$ phase from the $(1\times1)^1_1$ phase. Further details are discussed in the text.

VII. SUMMARY

We have fairly exhaustively determined the physical attributes of the $S=1$ Ising model with nearest-neighbor, pairwise interactions on the triangular lattice. In its most general form the Hamiltonian has three coupling parameters and two independent, spatially constant fields. We find $(\sqrt{3}\times\sqrt{3})$ ordered phases and (1×1) disordered

phases but no (2×2) phases in agreement with the results of a group-theoretical ground-state calculation. The three parameters give several topologically distinct classes of ground state diagrams in the k-l plane, especially for $j=-1$. The phase diagrams are strongly affected by the asymptotic behavior at large $-\mu_A$, $-\mu_B$, and $-d$. Much of the interesting phenomena occur at the intersection of these asymptotic phase boundaries at intermediate field strengths. We find either first-order transitions or no transition separating two ordered phases when they meet in this region. First-order boundaries separate the ordered phases from the disordered phases in the intermediate region, terminating the long hump of the ordered phase. If this first-order transition has a critical temperature lower than the asymptotic critical temperature of the second-order surface intersecting it then the second-order surface generally suffers more distortion. In the situations where two ordered phases intersect with no transition separating them, such as the $(\sqrt{3}\times\sqrt{3})^{2/3}_{-2/3}$ to $(\sqrt{3}\times\sqrt{3})^{1}_{-1/3}$ transition in model P,

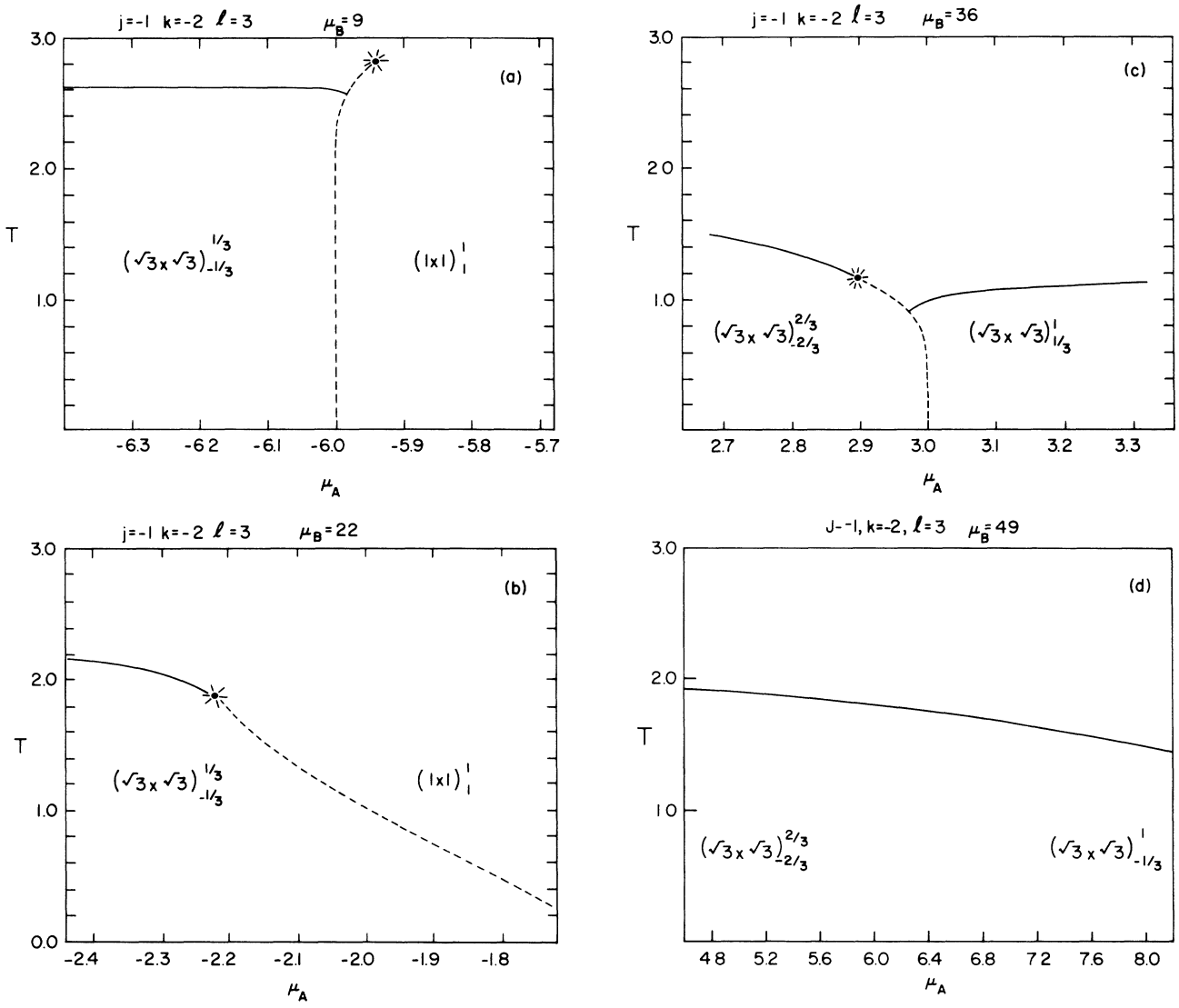

FIG. 5. Cross sections of model P across the first-order transition at constant μ_B. The μ_A ranges of these cross sections correspond to the horizontal bars indicated on Fig. 3(b). (a) Here, with the critical temperature for the first-order surface above that for the second-order surface, there is little distortion of the asymptotic shapes. The second-order surface terminates on the first-order surface at a critical endpoint. (b) The second-order surface is "pulled" down here and the first-order surface is "pulled" sideways. The asymptotic critical temperature for the second-order surface at large $-\mu_A$ is approximately 2.21. Our numerical accuracy is not sufficient here to determine whether the lines join at a tricritical point or with a critical point and a critical endpoint in close proximity. (c) The first-order line joins one second-order line at a tricritical point and meets another at a critical endpoint. Note the diminishing critical temperature for the first-order transitions. (d) Here there is no first-order transition except at zero temperature. The two asymptotic second-order surfaces join smoothly and continuously.

then the second-order surfaces join smoothly and continuously.

Overall, we find that the resulting phase diagrams are quite complicated, and the surfaces of first- and second-order phase transitions intersect along lines of multicritical points of various kinds. We find that this most general nearest-neighbor $S=1$ Ising model provides an unusually rich laboratory for studying a number of phase transitions, critical, and multicritical phenomena within the framework of one single model. At the same time the model is widely applicable to a number of interesting physical and chemical problems.

ACKNOWLEDGMENTS

The authors were supported by the Commonwealth of Pennsylvania's Ben Franklin partnership through the Advanced Technology Center of Southeastern Pennsylvania, a program of the University City Science Center. E.T.G. also acknowledges support in part by the Office of Naval Research Grant No. N00014-83-K-0382. P.A.R. acknowledges additional support from The Center for Materials Science and Technology and The Supercomputer Computations Research Institute at Florida State University.

---

*To whom correspondence should be addressed.

[1]E.g., P. A. Rikvold, K. Kaski, J. D. Gunton, and M. C. Yalabik, Phys. Rev. B **29**, 6285 (1984), and references cited therein.

[2]P. D. Beale, Phys. Rev. B **33**, 1717 (1986).

[3]W. Kinzel and M. Schick, Phys. Rev. B **23**, 3435 (1981); Y. Saito and G. Tabe, J. Phys. Soc. Jpn. **54**, 2955 (1985).

[4]N. C. Bartelt, T. L. Einstein, and L. D. Roelofs, Phys. Rev. B **34**, 1616 (1986); L. D. Roelofs, T. L. Einstein, N. C. Bartelt, and J. D. Shore, Surf. Sci. **176**, 295 (1986).

[5]P. A. Rikvold, J. B. Collins, G. D. Hansen, J. D. Gunton, Surf. Sci. (to be published).

[6]M. Blume, Phys. Rev. **141**, 517 (1966); H. W. Capel, Physica **32**, 966 (1966).

[7]M. Blume, V. J. Emergy, and R. B. Griffiths, Phys. Rev. A **4**, 1071 (1971).

[8]W. Selke and Y. M. Yeomans, J. Phys. A **16**, 2789 (1983); W. Selke, D. A. Huse, D. M. Kroll, J. Phys. A **17**, 3019 (1984); D. P. Landau and R. H. Swendsen, Phys. Rev. B **33**, 7700 (1986).

[9]J.-P. Legre, G. Albinet, J.-L. Firpo, and A.-M. S. Tremblay, Phys. Rev. A **30**, 2720 (1984).

[10]J.-P. Legre, J.-L. Firpo, and G. Albinet, Phys. Rev. A **31**, 1703 (1985); J.-L. Firpo, J.-P. Legre, A. G. Bois, and J. F. Baret, J. Chim. Phys. **81**, 113 (1984).

[11]Y. Saito, J. Chem. Phys. **74**, 713 (1981).

[12]M. Schick and Wei-Heng Shih, Phys. Rev. B **34**, 1797 (1986); Phys. Rev. Lett. **59**, 1205 (1987).

[13]D. A. Huckaby and J. M. Kowalski, J. Chem. Phys. **80**, 2163 (1984).

[14]D. H. Lee, J. D. Joannopoulos, J. W. Negele, and D. P. Landau, Phys. Rev. B **33**, 450 (1986).

[15]A. N. Berker and M. Wortis, Phys. Rev. B **14**, 4946 (1976).

[16]M. Kaufman, R. B. Griffiths, J. M. Yeomans, and M. E. Fisher, Phys. Rev. B **23**, 3448 (1981).

[17]J. M. Yeomans and M. E. Fisher, Phys. Rev. B **24**, 2825 (1981).

[18]F. C. Alcaraz, J. R. Drugowich de Felicio, R. Koberle, and J. F. Stilck, Phys. Rev. B **32**, 7469 (1985).

[19]B. C. Schardt, J. L. Stickney, D. A. Stern, A. Wieckowski, D. C. Zapien, and A. T. Hubbard, Surf. Sci. **175**, 520 (1986).

[20]E. Protopopoff and P. Marcus, Surf. Sci. **169**, L237 (1986).

[21]J.-P. Muscat, Phys. Rev. B **33**, 8136 (1986).

[22]E. Domany, M. Schick, J. S. Walker, and R. B. Griffiths, Phys. Rev. B **18**, 2209 (1978); M. Schick, Prog. Surf. Sci. **11**, 245 (1981).

[23]R. J. Baxter, *Exactly Solved Models in Statistical Mechanics* (Academic, London, 1982), Chap. 11.8.

[24]G. H. Wannier, Phys. Rev. **79**, 357 (1950).

[25]C. Domb, *Phase Transitions and Critical Phenomena* (Academic, London, 1974), Vol. 3, Chap. 6.

[26]S. Alexander, Phys. Lett. **54a**, 353 (1975).

[27]R. J. Baxter, J. Phys. A **13**, L61 (1980).

[28]R. J. Baxter, I. G. Enting, and S. K. Tsang, J. Stat. Phys. **22**, 465 (1980); Z. Racz, Phys. Rev. B **21**, 4012 (1980).

[29]B. D. Metcalf, Phys. Lett. **45A**, 1 (1973).

[30]A. Malakis, J. Phys. A **14**, 2767 (1981).

[31]C. Domb, Adv. Phys. **9**, 149 (1960).

[32]M. P. Nightingale, Physica A **83**, 561 (1976); Phys. Lett. **59a**, 486 (1977).